Fabrication of mirrors for the Magellan telescopes and the Large Binocular Telescope

H. M. Martin[a], R. G. Allen[a], J. H. Burge[b], L. R. Dettmann[a], D. A. Ketelsen[a], S. M. Miller[a] and J. M. Sasian[b]

[a]Steward Observatory, University of Arizona, Tucson, AZ 85721
[b]Optical Sciences Center, University of Arizona, Tucson, AZ 85721

ABSTRACT

We describe the fabrication and testing of the 6.5 m f/1.25 primary mirrors for the Magellan telescopes and the 8.4 m f/1.14 primary mirrors for the Large Binocular Telescope (LBT). These mirrors, along with the 6.5 m MMT primary, are the fastest and most aspheric large mirrors made. Steward Observatory developed special methods to polish and measure these and other fast mirrors. We use a stressed-lap polishing tool to fit the aspheric surface while providing strong passive smoothing, and computer-generated holograms to verify the measurement of up to 1.4 mm peak-to-valley asphericity to an accuracy of 0.01%. The Magellan mirrors are diffraction-limited at visible wavelengths, with surface accuracies of about 20 nm rms on active supports. We are currently polishing the first LBT primary mirror and preparing to make the thin shells for the LBT adaptive secondary mirrors.

Keywords: telescopes, optical fabrication, optical testing, aspheres

1. INTRODUCTION

The MMT and the two Magellan telescopes use 6.5 m honeycomb sandwich mirrors, cast and polished at the Steward Observatory Mirror Lab.[1,2] The Large Binocular Telescope, under construction on Mt. Graham in southeastern Arizona, will use two 8.4 m honeycomb sandwich mirrors on a common mount.[3] All of these mirrors are lightweighted by a factor of 5, giving them excellent stiffness and thermal response. They are also the fastest mirrors made for large telescopes—f/1.25 for the 6.5 m mirrors and f/1.14 for the 8.4 m mirrors—leading to short, stiff telescope structures and compact, economical enclosures.

These fast mirrors are highly aspheric and therefore present special challenges in optical fabrication and testing. Section 2 describes the techniques used. After figuring is completed, each mirror is installed in its active support cell, and support forces are optimized in the lab before the system is shipped to the telescope. Section 3 describes this process, and Section 4 gives the results for the Magellan mirrors in terms of surface accuracy and image quality. Section 5 describes the status of the fabrication of primary and secondary mirrors for the LBT.

2. FABRICATION AND TESTING

The casting and polishing processes have been described previously.[4,5] Briefly, we form the honeycomb sandwich mirror blank by spin-casting Ohara E6 borosilicate glass in a ceramic fiber mold. Hexagonal boxes in the mold form the cavities in the honeycomb, creating the structure illustrated in Figure 1. The maximum section thickness (the front facesheet) is 28 mm. Spinning the furnace while the glass is molten produces the parabolic surface to an accuracy of about 1 mm and eliminates the need to grind out 30 or 45 cm of solid glass for the 6.5 m or 8.4 m mirrors.

Large Ground-based Telescopes, Jacobus M. Oschmann, Larry M. Stepp, Editors,
Proceedings of SPIE Vol. 4837 (2003) © 2003 SPIE · 0277-786X/03/$15.00

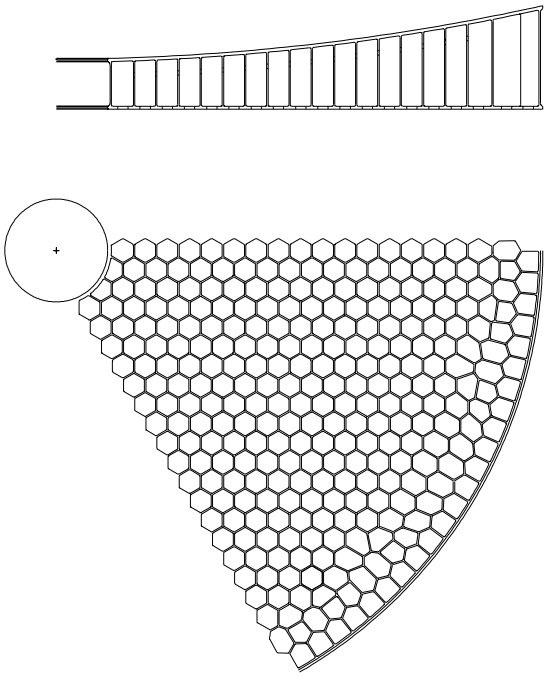

Figure 1. Honeycomb structure of the 8.4 m LBT mirrors. The mirror thickness varies from 437 mm at the inner edge to 894 mm at the outer edge. The back plate is 25 mm thick and the front plate 28 mm thick. Ribs 12 mm thick separate the hexagonal cavities, which have a center-to-center spacing of 192 mm.

We use an 8.4 m capacity numerically controlled mill with diamond tools to grind to the final dimensions and a front surface accuracy of 10 μm rms.[6] We polish the flat back surface in order to toughen it against impacts and allow visual inspection for internal flaws. At this point we bond to the back surface interfaces for the active support actuators, of which there are 104 for the 6.5 m mirrors and 160 for the 8.4 m mirrors. Most of the interfaces are two- or three-point loadspreaders giving a density of 8 support points per square meter on the mirror.

For loose-abrasive grinding and polishing, we use a polishing tool whose shape is actively controlled to match the varying curvature of the aspheric optical surface. This stressed lap, shown in Figure 2, was designed specifically for the highly aspheric surfaces of fast primary mirrors. A similar system about 1/4 the size is used for secondary mirrors up to 1.7 m in diameter. The lap shown in Figure 2 consists of an aluminum plate 50 mm thick and 1.5 m in diameter, with 18 moment-generating actuators around its perimeter to bend the plate elastically. The plate is faced with pitch on a layer of nylon that fills the sag between the flat plate and the concave mirror surface. The plate is stiff enough to provide strong passive smoothing of surface errors with amplitudes of 10 nm or more, on spatial scales up to 20-30 cm. We address large-scale axisymmetric figure errors by varying the lap's dwell time and rotation rate as a function of its radial position on the mirror. We address both symmetric and asymmetric figure errors by varying the polishing pressure and pressure gradients (radial and tangential), which are controlled dynamically by three actuators that apply lifting forces normal to the plate.

We use a 10.6 μm phase-shifting interferometer to measure during loose-abrasive grinding and early stages of polishing, then finish with a 633 nm interferometer. In both cases refractive null lenses compensate for the mirror's asphericity—810 μm peak-to-valley for the 6.5 m mirrors and 1.38 mm for the 8.4 m mirrors.[7,8] Each null lens is a substantial optical system. The visible null lens shown in Figure 3 is 1.6 m long and has high-quality lenses 220 mm and 290 mm in diameter.

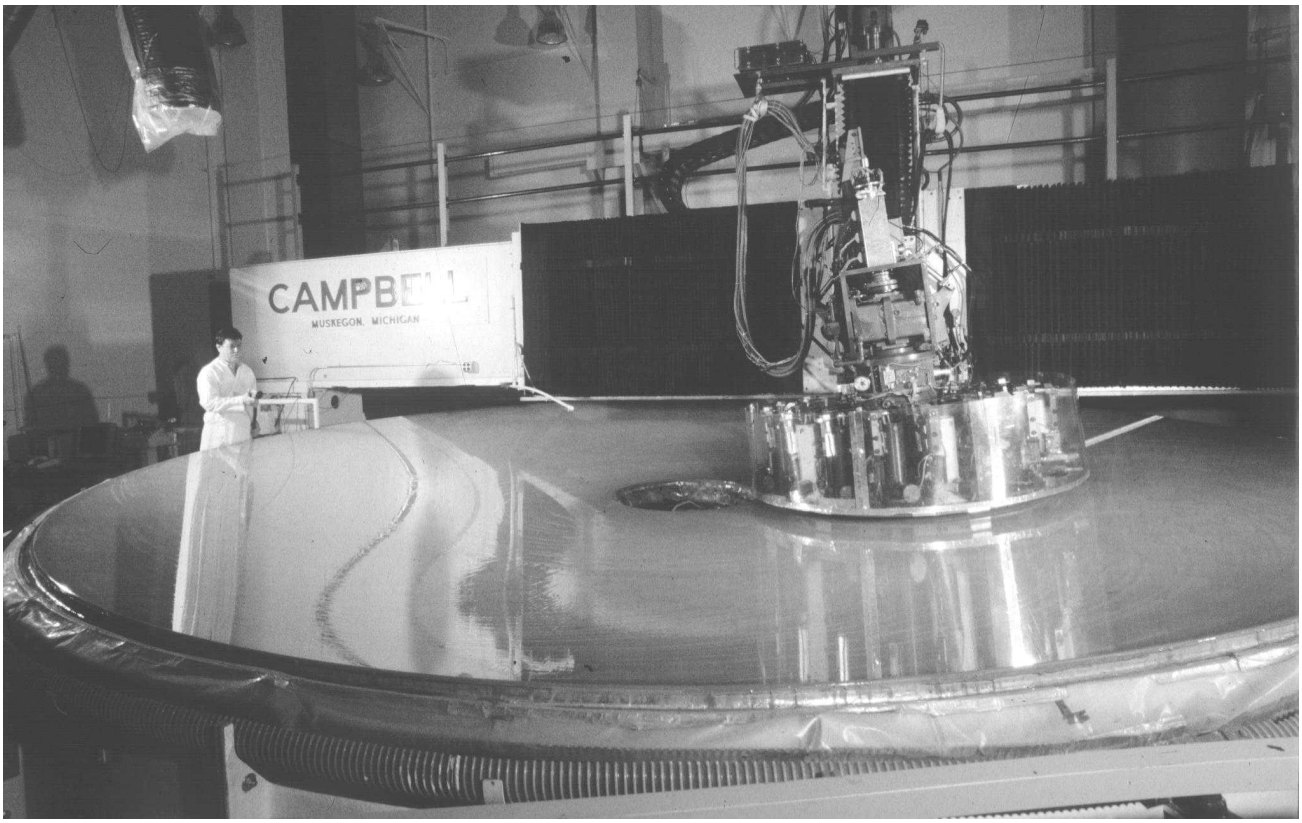

Figure 2. Stressed-lap polishing of a 6.5 m mirror. The lap bends continuously to match the local curvature of the f/1.25 mirror.

The goal is to measure the mirror's asphericity, or conic constant, to an accuracy of 0.01%. This measurement is critical to the telescope performance, so we have developed two independent measurements of the accuracy of the null lenses. Both work by mimicking a perfect primary mirror, that is, they send light back through the null lens as a perfect primary would. The ultimate standard for the measurement of the mirror is a computer-generated hologram which, when placed at the mirror's paraxial center of curvature, diffracts light back through the null lens. The second independent measurement works in the same way but by reflection from a diamond-turned aspheric mirror. Neither of the independent measurements can match the small-scale accuracy of the null lens, but the hologram is expected to be more accurate on large scales, while the diamond-turned mirror guarantees against gross errors and can help to resolve any dispute between the null lens and the hologram. Both tests are independent of the null lens; the designs of the hologram and diamond-turned mirror are based on the primary mirror, without reference to the null lens.

3. INTEGRATION AND SUPPORT OPTIMIZATION

Throughout the polishing process, each mirror rests on a set of passive hydraulic supports at the same locations as the telescope axial supports, with support forces calculated to minimize self-weight deflections. When polishing is complete, we install the mirror in its operational support cell with active pneumatic actuators.[9] Slight differences between the two sets of supports cause significant deflections of the mirror, so we adjust the active supports to minimize the wavefront error. We perform this optimization in terms of the mirror's natural bending modes, in order to minimize the actuator forces used to achieve a given improvement in wavefront error.[10] We start by correcting the softest bending mode, astigmatism, and continue through increasingly stiff modes until no significant improvement is achieved. While 101 bending modes are available for the Magellan mirrors—104 actuators less 3 constraints on net force and moments—

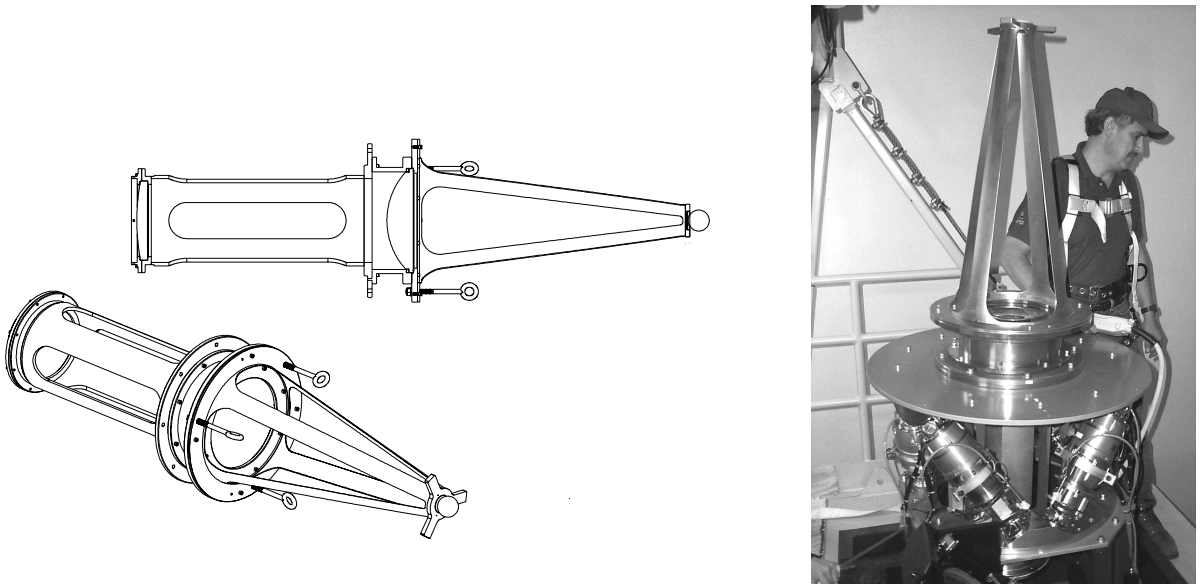

Figure 3. Three views of the visible wavelength null lens for the LBT mirrors. The small sphere is removable and is used to align the null lens with respect to a converging spherical wavefront from the interferometer (not shown). The aspheric compensation is done by the two lenses at the center and left side of the drawings. The overall length is 1.6 m. The entire system—interferometer and null lens—is aligned relative to the LBT mirror with the hexapod positioner shown in the photo.

we use between 20 and 30 modes in the optimization. There is little deflection present in higher modes, and correcting it requires larger forces that tend to leak into soft modes, making it difficult to converge on an optimum set of forces. Maximum correction forces are 30-45 N, 3-4.5% of the average gravity load.

The mirror is restricted to zenith pointing in the lab, so we only optimize the zenith-pointing component of axial forces. A similar optimization is performed in the Magellan telescopes at all elevation angles, using starlight as a reference wavefront measured with a Shack-Hartmann sensor. One advantage of optimizing first in the lab is that the stable conditions and more accurate measurements allow correction of somewhat higher spatial frequencies. Mid-spatial-frequency errors (above mode 15 or 20) due to the change in support mechanisms can be corrected once and for all in the lab and are not expected to change significantly in the telescope, while low-spatial-frequency errors that vary due to dynamic support errors, wind and temperature gradients are controlled by active optics in the telescope.

Optimization of support forces is based on the same interferometric wavefront measurements used during fabrication. We have the option of calculating or measuring the actuators' influence functions—the mirror deflections for a unit change in each actuator's force. We verified good agreement between the two during tests of the first 6.5 m mirror, and therefore use the calculated values which are free of noise and more easily obtained. During tests of the second Magellan mirror and its support system, we also measured the shapes and amplitudes of several bending modes, as shown in Figure 4. We applied force patterns corresponding to 5 of the 20 softest modes, and mode 29 which is significantly stiffer and is not used in the optimization. Table 1 lists the magnitude of applied forces and both predicted and measured deflections. Modes are labeled in order of increasing stiffness and are identified by the azimuthal symmetry and number of radial zero-crossings.

In all cases the amplitude of the desired mode is within 20% of the prediction, and within 8% for modes 1, 10, 12 and 13 which have better signal:noise. Any inaccuracy in the model of the mirror used to calculate influence functions and modal force patterns will cause some leakage into astigmatism. For the modes with better signal:noise this leakage is as much as 22% in deflection, i. e., astigmatism appears with an rms deflection of up to 22% of the rms deflection in the desired mode. But when one takes into account the stiffness of the modes—astigmatism has a much higher ratio of deflection to force—this represents less than 1% leakage in force. Even mode 29's 73% leakage in deflection represents less than 0.5% leakage in force.

Table 1. Measured response to modal force patterns

mode	radial zero-crossings	azimuthal symmetry	rms force (N)	predicted rms deflection (nm surface)	measured rms deflection (nm surface)	rms deflection in astigmatism (nm surface)
1	0	2	4	336	349	
10	1	2	120	338	335	75
12	0	5	120	296	274	27
13	0	5	120	272	267	36
17	1	3	120	158	138	28
29	1	5	120	64	52	47

4. RESULTS

Figures 5 and 6 and Table 2 summarize the results of figuring the Magellan mirrors and optimizing their support forces. Measurements of the mirrors on the passive polishing supports represent the accuracy achieved in polishing. These have astigmatism subtracted, as we make little effort to control this softest mode by figuring when it will be determined in the telescope by the active supports. Seidel spherical aberration is also subtracted because it is within the expected accuracy of the null lens and can be eliminated in the telescope by a small adjustment of the back focal distance. Measurements of the mirrors on the active telescope supports have no artificial correction. These results show that the Magellan mirrors can achieve approximately 20 nm rms surface error in the telescope. In practice, their surface accuracy will be limited by the wavefront measurements used to guide the active optics in the telescope.

Figure 7 shows encircled energy diagrams for the mirrors on the polishing and telescope supports, and Table 2 gives the image diameters containing 80% of the energy.. The diffraction calculation covers a 4″ field with 7.2 mas resolution at a wavelength of 500 nm. Encircled energy diagrams are given for perfect seeing and for 0.25″ seeing, calculated by convolving the mirror's PSF with that of the atmosphere. The mirrors are capable of better than 0.1″ images in perfect seeing, and cause a negligible degradation of images in 0.25″ seeing. The difference between the two mirror's encircled energies beyond 0.1" may be due in part to different imaging systems used to make the wavefront measurements.

5. OPTICS FOR THE LBT

Both LBT primary mirrors have been cast, at 8.4 m the largest mirrors ever made. The first is being polished with the same stressed-lap system used for the Magellan mirrors, with completion expected in late 2002. We will grind the second mirror as soon as we finish polishing the first. Polishing of the second mirror will be done with a new 8.4 m machine, to be installed in the Mirror Lab in early 2003. This second machine will relieve the bottleneck in the production of large honeycomb sandwich mirrors, nearly doubling the possible rate of production.

The LBT's secondary mirrors will be adaptive, based on the same design as the MMT adaptive secondary.[11,12] The concave reflecting surface is on a glass shell 1.6 mm thick and 910 mm in diameter. Its shape is controlled by 672 fast voice-coil actuators that suspend the shell about 40 μm away from a rigid glass reference body.

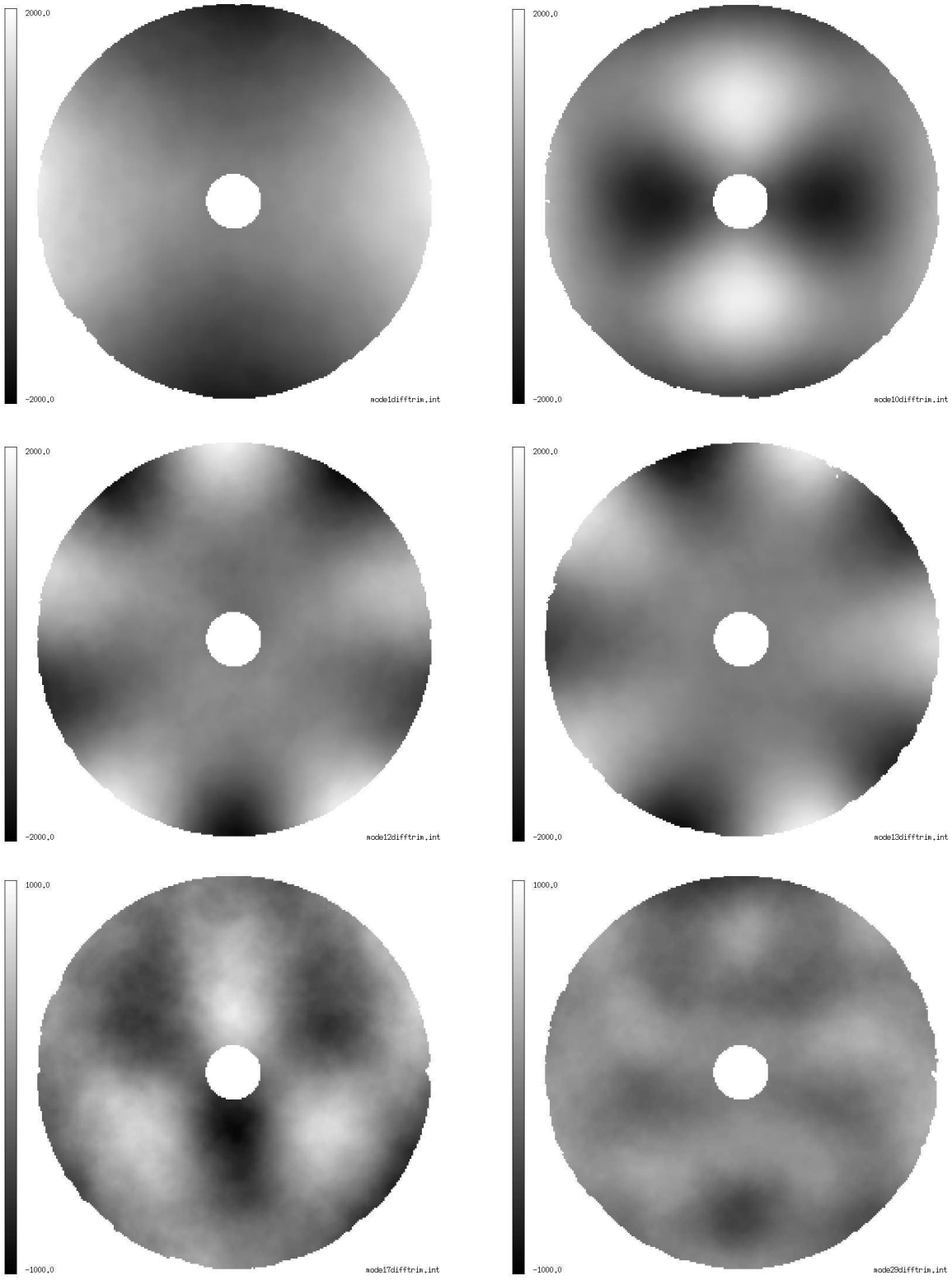

Figure 4. Measured bending modes induced by the active supports on the second Magellan primary mirror. Gray-level bars are labeled in nm of surface. The applied forces are listed in Table 1.

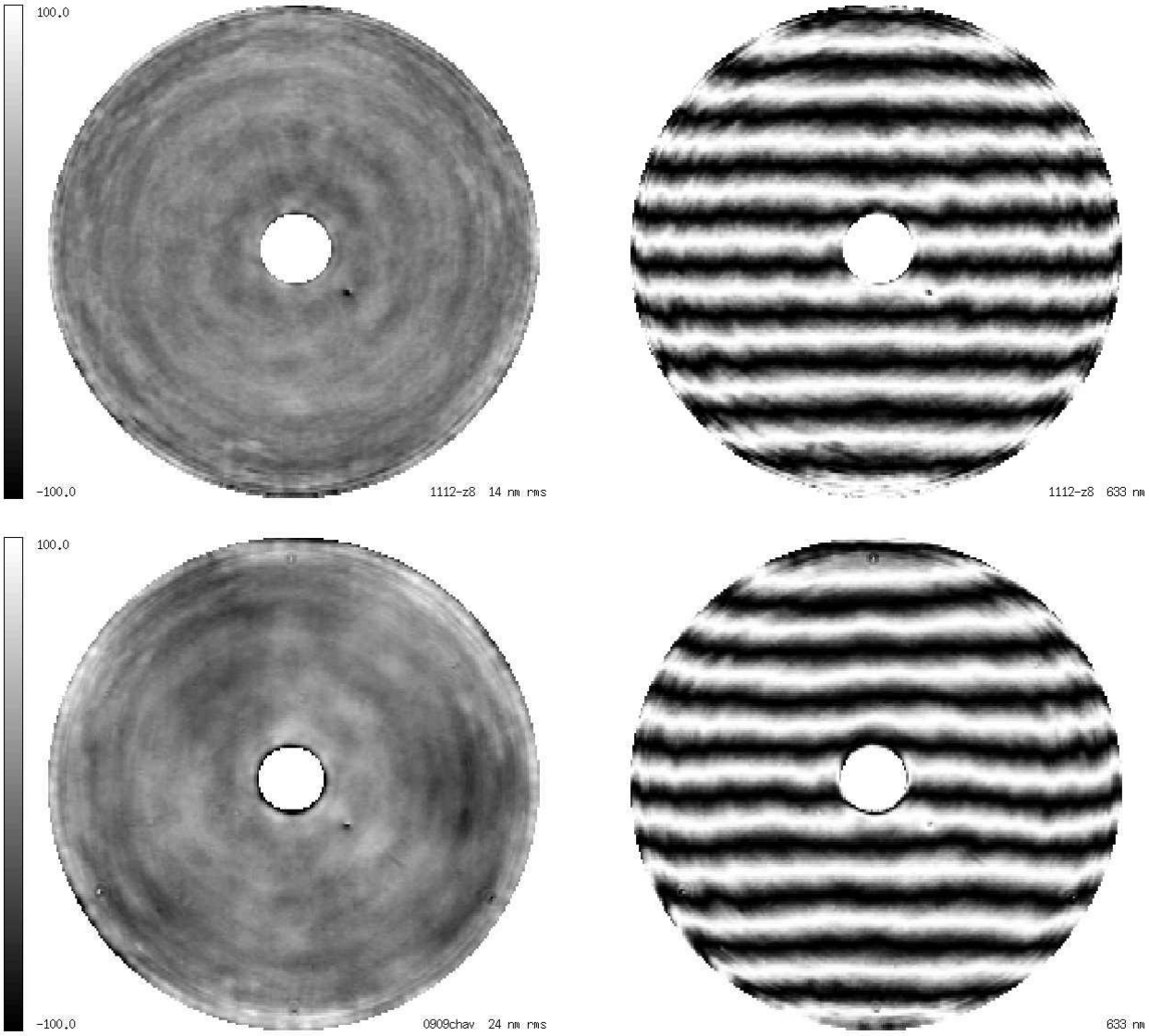

Figure 5. Grayscale surface maps and synthetic interference patterns for the first Magellan mirror. Grayscale bars are labeled in nm of surface; interference patterns are calculate for 633 nm. Top: at completion of polishing, with mirror on passive polishing support; astigmatism and spherical aberration have been subtracted. Bottom: with mirror on active telescope support, after optimization of support forces; no aberrations have been subtracted.

We have developed a method of figuring the thin shells through experience with a number of prototypes and the MMT adaptive secondary shell.[13] Two factors influence the method. First, the secondary, like the primary, is very aspheric (130 μm peak-to-valley departure from the best-fit sphere), so we want to use the stressed-lap polishing system, which is best suited to rigid mirrors. Therefore the secondary should at least act like a rigid mirror while we polish the optical surface. Second, low- and mid-spatial-frequency errors will be controlled entirely by the actuators, and the figuring process need only achieve smoothness on small scales. We made the MMT shell by attaching the thin shell to a rigid blocking body, using a thin layer of pitch to bond them. It proved difficult to maintain uniform pressure at the pitch interface, so we have modified the process for the LBT shells. We will polish and figure the optical surface on a relatively thick piece of Zerodur, then thin it by grinding glass from the rear surface. The optical surface will deform

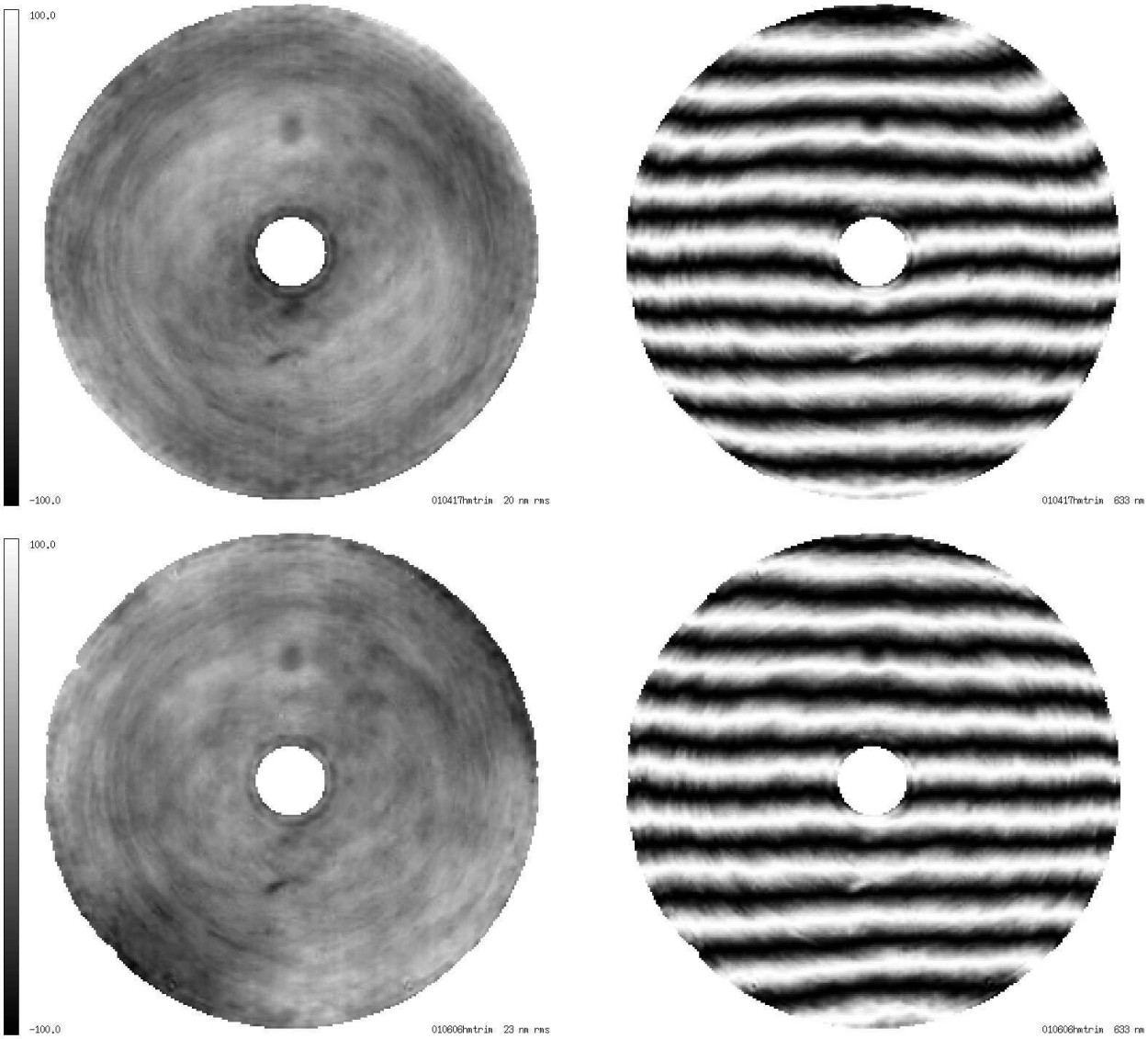

Figure 6. Grayscale surface maps and synthetic interference patterns for the second Magellan mirror. Grayscale bars are labeled in nm of surface; interference patterns are calculate for 633 nm. Top: at completion of polishing, with mirror on passive polishing support; astigmatism and spherical aberration have been subtracted. Bottom: with mirror on active telescope support, after optimization of support forces; no aberrations have been subtracted.

with the removal of about 100 mm of glass and its internal stress, but we expect the deformations to be on sufficiently large scales that they will be corrected by the actuators with modest forces.

Table 2. Surface accuracy and image quality for Magellan mirrors on polishing support and telescope support

	rms surface error (nm)	diameter containing 80% of light at 500 nm	
		perfect seeing	0.25″ seeing
perfect mirror	0	0.05″	0.49″
Magellan 1, polishing support	14	0.06″	0.54″
Magellan 1, telescope support	24	0.11″	0.54″
Magellan 2, polishing support	19	0.08″	0.52″
Magellan 2, telescope support	22	0.07″	0.52″

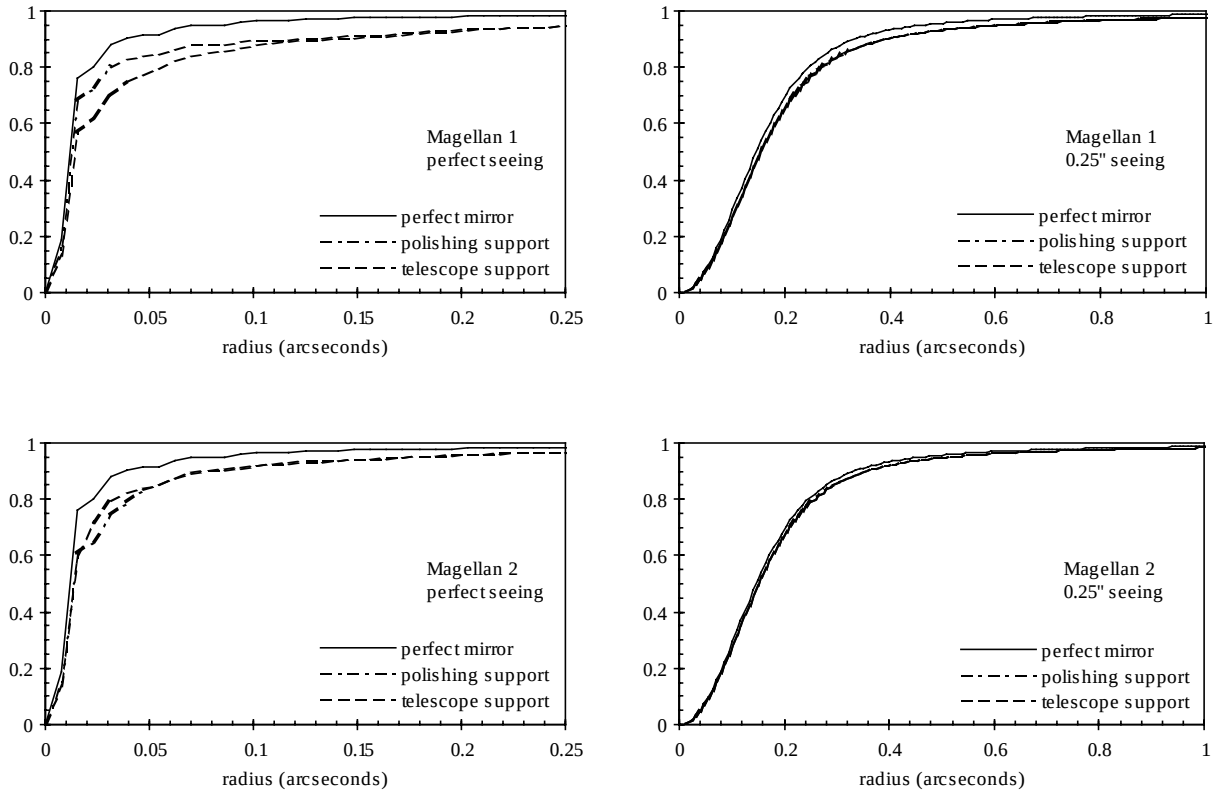

Figure 7. Encircled energy as a function of radius for the Magellan mirrors on the passive polishing support and on the active telescope support. Astigmatism and spherical aberration were subtracted from the wavefronts measured on the passive support, but no correction was made to the wavefronts measured on the active support. Wavelength is 500 nm.

6. CONCLUSION

The fabrication process for fast honeycomb sandwich mirrors has reached a high level of maturity with the manufacture of two 6.5 m f/1.25 primary mirrors for the Magellan telescopes. The mirrors and their active support systems can produce diffraction-limited images in the lab, and the mechanical and thermal properties of these mirrors promise excellent performance in the telescope as well. Mirrors for the LBT are in production and are expected to achieve similar performance.

REFERENCES

1. S. C. West, S. Callahan, F. H. Chaffee, W. B. Davison, S. T. DeRigne, D. G. Fabricant, C. B. Foltz, J. M. Hill, R. H. Nagel, A. D. Poyner, J. T. Williams, "Toward first light for the 6.5-m MMT telescope", in *Optical Telescopes of Today and Tomorrow: Following in the Direction of Tycho Brahe*, ed. A. Ardeberg, Proc. SPIE 2871, p. 38 (1997).
2. S. A. Shectman, "The Magellan Project", in *Telescope Structures, Enclosures, Controls, Assembly/Integration/Validation, and Commissioning*, ed. T. Sebring, T. Andersen, Proc. SPIE 4004, p. 47 (2000).
3. J. M. Hill, P. Salinari, "The Large Binocular Telescope Project, in *Telescope Structures, Enclosures, Controls, Assembly/Integration/Validation, and Commissioning*, ed. T. Sebring, T. Andersen, Proc. SPIE 4004, p. 36 (2000).
4. B. H. Olbert, J. R. P. Angel, J. M. Hill, S. F. Hinman, "Casting 6.5-meter mirrors for the MMT conversion and Magellan", in *Advanced Technology Optical Telescopes V*, ed. L. M. Stepp, Proc. SPIE 2199, p. 144 (1994).
5. H. M. Martin, R. G. Allen, B. Cuerden, S. T. DeRigne, L. R. Dettmann, D. A. Ketelsen, S. M. Miller, G. Parodi and S. Warner, "Primary mirror system for the first Magellan telescope", *Optical Design, Materials, Fabrication, and Maintenance*, ed. P. Dierickx, Proc. SPIE 4003, p. 2 (2000).
6. D. A. Ketelsen, W. B. Davison, S. T. DeRigne, W. C. Kittrell, "Machine for complete fabrication of 8-m class mirrors", in *Advanced Technology Optical Telescopes V*, ed. L. M. Stepp, Proc. SPIE 2199, p. 651 (1994).
7. J. H. Burge, D. S. Anderson, D. A. Ketelsen, S. C. West, "Null test optics for the MMT and Magellan 6.5-m f/1.25 primary mirrors", in *Advanced Technology Optical Telescopes V*, ed. L. M. Stepp, Proc. SPIE 2199, p. 658 (1994).
8. J. M. Sasian, S. A. Lerner, J. H. Burge and H. M. Martin, "Design, tolerancing, and certification of a null corrector to test 8.4-m mirrors", *Optical Fabrication and Testing*, ed. R. Geyl, Proc. SPIE 3739, p. 444 (1999).
9. P. M. Gray, J. M. Hill, W. B. Davison, S. P. Callahan, J. T. Williams, "Support of large borosilicate honeycomb mirrors", in *Advanced Technology Optical Telescopes V*, ed. L. M. Stepp, Proc. SPIE 2199, p. 691 (1994).
10. H. M. Martin, S. P. Callahan, B. Cuerden, W. B. Davison, S. T. DeRigne, L. R. Dettmann, G. Parodi, T. J. Trebisky, S. C. West and J. T. Williams, "Active supports and force optimization for the MMT primary mirror", *Advanced Technology Optical/IR Telescopes VI*, ed. L. M. Stepp, Proc. SPIE 3352, p. 412 (1998).
11. M. Lloyd-Hart, F. Wildi, H. Martin, P. McGuire, M. Kenworthy, R. Johnson, B. Fitz-Patrick, G. Angeli, S. Miller, and R. Angel, "Adaptive optics at the 6.5 m MMT", *Adaptive Optical Systems Technology*, ed. P. L. Wizinowich, Proc. SPIE 4007, p. 167 (2000).
12. A. Riccardi, G. Brusa, V. Biliotti, C. Del Vecchio, P. Salinari, P. Stefanini, P. Mantegazza, R. Biasi, M. Andrighettoni, C. Franchini, D. Gallieni, M. Lloyd-Hart, P. C. McGuire, S. M. Miller and H. M. Martin, "The adaptive secondary mirror for the 6.5m conversion of the Multiple Mirror Telescope: latest laboratory test results of the P36 prototype", *Adaptive Optical Systems Technology*, ed. P. L. Wizinowich, Proc. SPIE 4007, p. 524 (2000).
13. H. M. Martin, J. H. Burge, C. Del Vecchio, L. R. Dettmann, S. M. Miller, B. Smith and F. Wildi, "Optical fabrication of the MMT adaptive secondary mirror", *Adaptive Optical Systems Technology*, ed. P. L. Wizinowich, Proc. SPIE 4007, p. 502 (2000).